Available online at www.sciencedirect.com
ScienceDirect
Scripta Materialia 59 (2008) 1263–1266
Scripta MATERIALIA
www.elsevier.com/locate/scriptamat

Local transformation strain measurements in precipitated NiTi single crystals

Christos Efstathiou* and Huseyin Sehitoglu

Department of Mechanical Science and Engineering, University of Illinois at Urbana Champaign, 1206 W. Green Street, Urbana, IL 61801, USA

Received 7 August 2008; revised 20 August 2008; accepted 24 August 2008
Available online 9 September 2008

The objective of this work was to determine the effect of composition on the local transformation strain in NiTi single crystals. Using in situ digital image correlation to obtain full-field strain measurements, we revealed that increasing Ni concentration and precipitate volume fraction results in smaller local transformation strains. Comparison of the local strain measurements to theoretical calculations indicated that detwinning strains are limited in Ni-rich compositions. It was also found that the Ni-rich compositions displayed a more homogeneous transformation.

Keywords: Digital image correlation; NiTi; Martensitic transformation; Shape memory alloy (SMA)

NiTi is perhaps the most successful shape memory alloy (SMA) used in practical applications. One reason for its success is that its transformation temperatures are easily tailored by aging. Aging can create 10–700 nm Ti_3Ni_4 precipitates with volume fractions of up to 20% in Ni-rich NiTi alloys [1,2]. By controlling the aging temperature and time, precipitates can be coherent, semicoherent or incoherent. Aging NiTi to form different precipitate sizes has benefits that include increased austenite yield strength, enhanced fatigue properties, two-way shape memory effect, and pseudoelasticity. Pseudoelasticity is a desirable property for SMAs because large strains can be recovered upon unloading. Although precipitates make pseudoelasticity possible, they effectively reduce the maximum transformation strain since they are untransformable. Additionally, it has been reported that precipitates may restrict the detwinning process [3], which can reduce the maximum transformation strain by up to 4% in the [111] orientation, or in polycrystals. The focus of this work is to provide direct experimental evidence of the effect of precipitates on the local transformation strain in low-, medium- and high-Ni content near-equiatomic NiTi alloys.

By utilizing digital image correlation (DIC), a full-field deformation measurement technique, we are able to identify that the presence of larger volume fractions of precipitates reduces the local transformation strain. Utilizing DIC allows several additional features of the phase transformation to be characterized, such as the spatial heterogeneity of the transformation, the transformation interface sharpness, and the uniformity of the strain within the transformed regions.

Single-crystal samples were grown using the Bridgman technique in an inert gas atmosphere. The loading axis of the single crystal was determined as [111] using Laue back-scatter diffraction patterns. The three compositions investigated were Ti–50.1% Ni, Ti–50.8% Ni and Ti–51.5% Ni (at.%). The Ti–50.8% Ni and Ti–51.5% Ni compositions will be referred to the Ni-rich compositions. The specimens were solutionized at 1000 C for 2 h in an inert gas atmosphere and subsequently aged at 550 °C for 1.5 h. The transformation temperatures for these materials are listed in Table 1.

The aged microstructure for each composition is shown in Figure 1 [4]. All compositions display approximately 500 nm Ti_3Ni_4 precipitates, but higher precipitate volume fractions (approximately 20%) and spatial uniformity exist in the Ni-rich compositions. Single-crystal defects such as dendrites and low-angle tilt boundaries have been reported by Wagoner et al. [5], and were deemed responsible for the nonuniform distribution of precipitates in the low-Ni alloy. We note that the precipitates do not transform to martensite. It is therefore expected that the experimental transformation

* Corresponding author. Tel.: +1 217 333 3859; fax: +1 217 244 6534; e-mail: efstathi@uiuc.edu

1359-6462/$ - see front matter © 2008 Acta Materialia Inc. Published by Elsevier Ltd. All rights reserved.
doi:10.1016/j.scriptamat.2008.08.030

Table 1. Transformation temperatures (°C) for the three compositions

Ni%	M_s	M_f	A_s	A_f
50.1	−10	−30	−12	7
50.8	−40	−50	−10	0
51.5	−45	−55	−13	−1

strain should be smaller than the theoretical values. The theoretical transformation strain for a precipitate-free alloy loaded in tension along the [111] crystallographic orientation was reported in Ref. [6] as approximately 6% for a Type II-1 twin, and approximately 10% after detwinning strains are accounted for (see Table 2). Table 2 includes estimates of the theoretical transformation strains for the aged material which contains 20% precipitate volume fraction. In addition to reducing the available material for transformation, precipitates may serve as obstacles to detwinning thus further reducing the local transformation strain.

Mechanical testing was conducted on a Materials Test Systems servohydraulic load frame. Nominal strains were measured with a miniature extensometer (5 mm gage length) to produce the nominal stress–strain curves. Strain rates were of the order of 10^{-4} s^{-1} to minimize both the rate effects and temperature changes during the experiments. All experiments were conducted at 25 °C.

In situ macroscopic observations were used to investigate the evolution of the transformation. Images were captured with an IMI model IMB-202FT CCD camera (1600 × 1200 pixels). A Navitar optical lens was used for macroscopic observations at low magnification that generated a resolution of 265 pixels mm^{-1}. DIC was performed on approximately 1.6 × 5 mm regions of interest to determine the local strain field during loading and unloading. Full-field measurements of both in-plane displacement components were obtained using DIC. The DIC technique measures displacement fields by tracking a random speckle pattern on the specimen surface [7]. Speckle patterns were applied to the surface of polished specimens using an Iwata Micron B airbrush. To perform DIC, a region of interest is selected in the reference image and divided into small square regions called subsets. Each subset represented a square region approximately 200 × 200 μm. Approximately 6000 subsets were used to create the strain fields. The average pixel intensity in each subset is calculated, and regions with the same intensity are sought in the deformed image. In order to find the location of a deformed subset and its shape change, optimization techniques are employed in which values of displacement and linear displacement gradients of a subset are obtained. For each subset, these values are adjusted until the difference in pixel intensity between the reference and deformed subsets is a minimum. The resulting displacement field is then differentiated to obtain the strain field according to the central difference scheme. Commercially available software (Vic2d) from Correlated Solutions was used to perform the image correlation and the strain calculations. Further details on the application of DIC can be found in Ref. [7] and a general background on DIC is given in Ref. [8].

Figure 2 shows the nominal stress–strain curve and three representative strain fields during the propagation of the transformation front in Ti–50.1% Ni. At early stages of deformation (shown in Fig. 2a), the front emerges at the top of the sample in a localized manner while the majority of the DIC region of interest has not transformed. With increased deformation, Figure 2b, the transformation front becomes well defined with a sharp interface and two distinct regions identified by the green and red color contours. The green region represents strains of the order of 6%, whereas the red region represents strains of the order of 10%. Note that these strain levels agree with the theoretical transformation strains reported for correspondent variant pair (CVP) strain, and CVP + detwinning strain, respectively (shown in Table 2). With further deformation, shown in Figure 2c, the transformation front continues to propagate while generating a domain behind the main front which has not completely detwinned. This is evidenced by the small green region surrounded by the red region (see arrow in Fig. 2c).

Figure 3 shows the nominal stress–strain curve and the representative strain fields during the front propagation in the Ti–50.8% Ni material. In Figure 3a the transformation occurs in a slightly more homogeneous manner compared to the Ti–50.1% Ni alloy, and the front appears inclined at a higher angle to the applied loading direction. With increased deformation, Figure 3b, a second transformation front appears at the top of the sample. At this stage of the deformation, a narrow red region is apparent within the lower transformation front with approximately 7% strain. This strain exceeds the theoretical CVP strain and indicates that partial det-

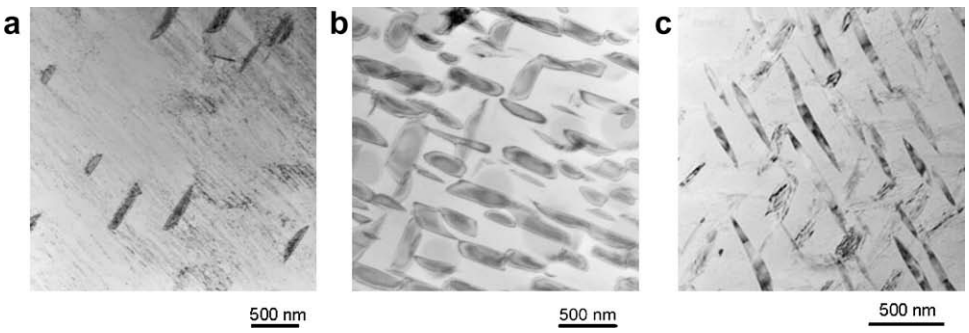

Figure 1. Transmission electron micrographs showing precipitate distribution for (a) Ti–50.1% Ni, (b) Ti–50.8% Ni, (c) Ti–51.5% Ni [4].

Table 2. Theoretical and measured transformation strains for the [111] crystallographic orientation loaded in tension

Material	Maximum transformation strain (%)
Precipitate free [6]	6.0/10.3
20% V_f precipitates	4.8/8.2
50.1 Ni%	10.0
50.8 Ni%	7.0
51.5 Ni%	4.0

The theoretical transformation strains are listed for precipitate-free material, and for material containing 20% precipitate volume fraction. Note both the CVP and CVP + detwinning strain magnitudes are provided from Ref. [6] for the precipitate-free material. For a precipitate volume fraction of approximately 20%, the expected transformation strains are 20% smaller than for the precipitate-free material since the precipitates do not transform. The maximum measured transformation strain, obtained from the strain fields, is included for each composition to identify if detwinning is present.

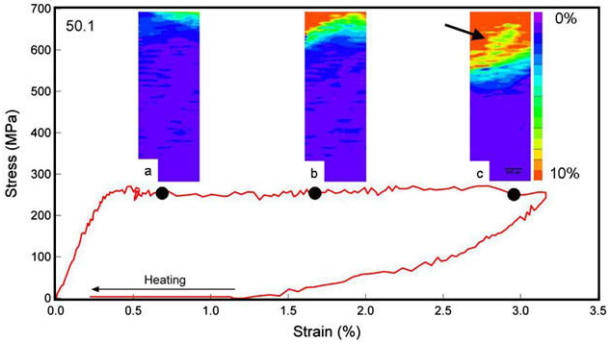

Figure 2. The nominal stress–strain curve, and the strain fields for Ti–50.1% Ni. The strain fields show the transformation front motion during increased deformation from points (a–c). The strain field is approximately 1.7 mm wide.

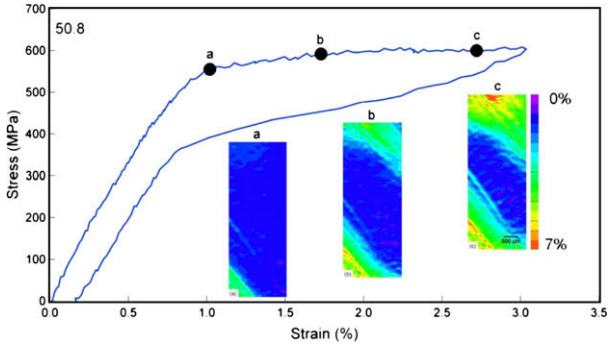

Figure 3. The nominal stress–strain curve, and the strain fields for Ti–50.8% Ni showing the transformation front motion during increased deformation from points (a–c). The strain field is approximately 2.0 mm wide.

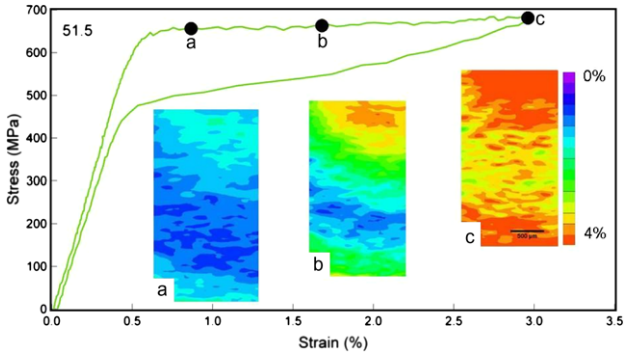

Figure 4. The nominal stress–strain curve, and the strain fields for Ti–51.5% Ni showing the transformation front motion during increased deformation from points (a–c). The strain field is approximately 1.4 mm wide.

winning is obtained in this composition. With further deformation, the fronts propagate toward the center of the sample (shown in Fig. 3c) while generating approximately 4% strain, and again some narrow detwinned regions form with approximately 7% strain. Note that the transformation interface approaching the top of the specimen appears less sharp compared to the Ti–50.1% Ni material, and is inclined at two different angles to the loading direction. These two angles (shown by the dashed lines in Fig. 3c) are the result of the interaction of two martensite CVPs.

Figure 4 shows the nominal stress–strain curve and the strain fields during the front propagation in the Ti–51.5% Ni alloy. In this alloy the transformation is noticeably more homogeneous, and the interface is considerably more diffuse. This alloy displays an apparent "curved" transformation interface which indicates multiple martensite CVP formation. The transformed areas do not display strains greater than approximately 4%, suggesting that detwinning strains are curtailed in this composition. Also noteworthy is the uniformity of the transformation strain within the transformed regions. Although not shown for all three alloys, unloading generates the reverse front propagation.

The strain fields presented in Figures 2–4 indicate significantly smaller local transformation strains for the Ni-rich alloys. The Ni-rich alloys both possess a higher precipitate volume fraction (Fig. 1) compared to the low-Ni alloy, and since the precipitates are untransformable it is expected that the transformation strains would be smaller in the aged Ni-rich alloys. Considering a precipitate volume fraction (or untransformable material volume) of approximately 20% for the Ni-rich alloys, it would be expected that the maximum CVP strain would be 4.8%, and the maximum CVP + detwinning strain would be 8.2% as shown in Table 2. Recall that the Ti–50.8% Ni alloy displayed narrow regions of approximately 7% strain (Fig. 3c) which is larger than the CVP strain, and approaches the CVP + detwinning strain of 8%. Thus detwinning is not exclusively found in precipitate-free low-Ni alloy; it is also present in the heavily precipitated Ti–50.8% Ni alloy. Although detwinning is present in the precipitated Ti–50.8% Ni alloy, it does not appear in the Ti–51.5% Ni alloy. The reason for this is probably a combination of several factors, including a high critical transformation stress which leads to fracture above 3% nominal strain, and multiple martensite CVP formation. The reduced mobility of twin boundaries due to the interaction of martensite CVPs could curtail the detwinning process and reduce the maximum transformation strain [3].

Transformation interface characteristics were also notably different for the three alloys. For the Ni-rich al-

loys, the interface was more diffuse and displayed a deviation from a flat interface. The apparent "curved" transformation interface, found in the heavily precipitated alloys, points to multiple CVP formation (Figs. 3c and 4c). This is distinctly different from the single CVP (Fig. 2c) found in the nearly precipitate-free low-Ni alloy. Although the martensite is stress-induced and expected to form a single CVP, the formation of multiple CVPs due to local precipitate stress fields can occur in these aged Ni-rich alloys, and has been reported by Hamilton et al. [4].

The heterogeneity of the strain field was dependent on the Ni concentration. A heterogeneous transformation was found in the low-Ni alloy which displayed a single front at the top of the sample shown in Figure 2c. However, at higher Ni concentrations and precipitate volume fractions, we found a more homogeneous transformation with several fronts forming and their boundaries less defined (see Fig. 4c). An explanation for this behavior is related to the different precipitate structures in these alloys. Precipitates serve as martensite nucleation sites, and it is expected that the heavily precipitated microstructure found in the Ni-rich alloys would nucleate martensite homogeneously throughout the sample volume with deformation. In contrast, the heterogeneous precipitate distribution in the low-Ni alloy would promote an isolated transformation that manifests into a transformation front which propagates with deformation.

Another transformation characteristic which was altered by the Ni concentration was the uniformity of the transformation strain. The strain within the transformed region generally appeared more uniform for higher Ni content alloys. This effect is most evident by comparing the strain field for the low-Ni alloy in Figure 2c to the strain field in the high-Ni alloy in Figure 4c. It was noted that, in the low-Ni alloy, a small domain did not detwin, resulting in nearly half the transformation strain (see arrow in Fig. 2c). This identifies that the local driving force differs depending on the composition or the local defects such as dendrites or low-angle tilt boundaries which have been reported for this alloy [5]. In the high-Ni alloy, the strains behind the main transformation front (Fig. 4c) are fairly uniform and suggest a more homogeneous microstructure and local transformation driving force. This observation is consistent with reports for aged Ni-rich alloys [4].

In summary, the results presented in this work underscore the role of precipitates in reducing transformation strains. The reason for the reduced transformation strain in the Ni-rich alloys was attributed to the smaller available material volume for the transformation, and the interaction of multiple martensite CVPs which results in incomplete detwinning. We determined that with a higher volume fraction of precipitates, the transformation fronts become more diffuse and spatially homogeneous.

The work was supported by the NSF Grant No. CMS-0428428, NSF DMR 08-03270, and Mechanical Systems and US-Italy Cooperative Research Program NSF OIS O4-37345. The single crystals were obtained from Prof. Y. Chumlyakov of Tomsk State University.

[1] H. Sehitoglu, J. Jun, X.Y. Zhang, I. Karaman, Y. Chumlyakov, H.J. Maier, K. Gall, Acta Mater. 3609 (2001) 49.
[2] K. Gall, H.J. Maier, Acta Mater. 4643 (2002) 50.
[3] T.E. Buchheit, J.A. Wert, Metall. Mater. Trans. 2383 (1994) 25A.
[4] R.F. Hamilton, H. Sehitoglu, Y. Chumlyakov, H.J. Maier, Acta Mater. 3383 (2004) 52.
[5] A.J. Wagoner, R.F. Hamilton, H. Sehitoglu, G. Biallas, H.J. Maier, Y.I. Chumlyakov, H.S. Woo, Metall. Mater. Trans. 919 (2005) 36A.
[6] H. Sehitoglu, R.F. Hamilton, D. Canadinc, X.Y. Zhang, K. Gall, I. Karaman, Y. Chumlyakov, H.J. Maier, Metall. Mater. Trans. 5 (2003) 34A.
[7] T. Chu, W.F. Ranson, M.A. Sutton, W.H. Peters, Exp. Mech. 232 (1985) 25.
[8] J.W. Dally, W.F. Riley, Experimental Stress Analysis, College House Enterprises, Knoxville, TN, 2005.